# Strain-dependent Dzyaloshinskii-Moriya interaction in a ferromagnet/heavy-metal bilayer

O. G. Udalov [1,2,3] and I. S. Beloborodov[1]

[1]*Department of Physics and Astronomy, California State University Northridge, Northridge, California 91330, USA*

[2]*Institute for Physics of Microstructures RAS, Nizhny Novgorod 603950, Russia*

[3]*Lobachevsky State University of Nizhny Novgorod, Nizhny Novgorod 603950, Russia*

(Received 6 July 2020; revised 21 August 2020; accepted 1 October 2020; published 15 October 2020)

We study the dependence of the Dzyaloshinskii-Moria interaction (DMI) using the *s-d* model in the bilayer ferromagnet/heavy-metal system on the mechanical strain applied to the system. We show that DMI is sensitive to the strain perpendicular to the film plane. It can vary 40% under the strain of 0.3%. Such a strong variation is in agreement with recent experiment [Phys. Rev. Lett. **124**, 157202 (2020)]. The DMI coefficient variation is mostly related to the change of the distance between heavy-metal atomic planes under the strain. Changing the in-plane distance between the heavy-metal ions does not produce strong variation of DMI. Anisotropy of the DMI interaction may appear if the strain is anisotropic in the plane of the bilayer. The DMI anisotropy is related to the anisotropy of the electron effective mass in the film plane induced by the strain.

DOI: 10.1103/PhysRevB.102.134422

## I. INTRODUCTION

Artificial multilayer structures with alternating ferromagnetic (FM) and heavy-metal (HM) layers get into focus of many groups nowadays [1–10]. Such structures host skyrmions which are considered as the next generation magnetic object for information storage and processing [11–16]. The stability of the skyrmions is provided by the Dzyaloshinskii-Moriya interaction (DMI). Therefore, many efforts were spent on studying this interaction. Control of the DMI with an external stimulus is one of the key issue [17,18] since it promises the skyrmion manipulation. The DMI can be controlled via charge accumulation in the system HM/FM/insulator [19–21]. When voltage is applied across the insulating layer the charge accumulation occurs in the FM layer leading to DMI variations. Recent experiments show that strain can essentially influence the DMI [22]. Theoretical explanation of this effect is lacking. In the present paper we propose a model for strain-dependent DMI in the FM/HM bilayer system.

Following a Fert and Levy idea [23] the DMI appears due to triple coupling of conduction electrons to spin-orbit (SO) impurity and two FM ions. According to Ref. [23] the dependence of the DMI on the distance between two ions is similar to the Ruderman-Kittel-Kasuya-Yosida (RKKY) interaction showing short-period oscillations. So, one can expect that the DMI interaction is sensitive to a strain applied to bilayer FM/HM film. Based on this idea we calculate the DMI as a function of strain applied to the system and show that it indeed depends on the mechanical deformation.

Recently, the DMI was considered using a perturbation theory in Ref. [24]. In this work the SO and the *s-d* exchange interactions were treated as a perturbation. Several other models were used to describe the DMI in the FM/HM system. In Refs. [25–27] the bilayer system was changed by the effective uniform medium with Rashba interaction.

Direct application of the Levy-Fert formula for FM/HM system was used in Refs. [28,29]. The authors averaged the Levy-Fert expression for ion-ion interaction over all HM atoms in the system and obtained the DMI constant. Generally, the same approach can be used to study the influence of strain on the DMI since the distance between ions directly enters into the expression for two ion interaction. However, it is not clear to what extent the result for the interaction of two magnetic ions via a spin-orbit impurity in a nonmagnetic metal can be applied to the bilayer system. In the Levy-Fert approach the electrons mediating the DMI are free ones. The exchange interaction is considered as a perturbation. This is not the case for the FM/HM system where the exchange coupling is usually strong and essentially modifies electron energy spectrum and wave functions. Moreover, the applied strain can also change the energy quantization in the system which can modify the DMI. This cannot be taken into account using the approach of Ref. [28]. Therefore, here we generalize the Levy-Fert approach for a bilayer system following a more regular procedure.

The paper is organized as follows. First, we introduce the model of a ferromagnetic/heavy-metal bilayer. Next, we calculate the DMI and discuss general properties of the interfacial DMI in Sec. III. In Sec. IV we consider the dependence of the DMI on applied mechanical strain. Finally, we compare our results with recent experimental data and discuss limits of our model in Sec. V.

## II. THE MODEL

Consider the system consisting of two layers with an interface at the plane $y = 0$ (see Fig. 1). The upper part of the system ($y < 0$) represents a FM material and the bottom part is the material with **a** spin-orbit interaction [heavy metal (HM)]. The FM layer has thickness $d_{\mathrm{FM}}$, the HM layer has thickness

 

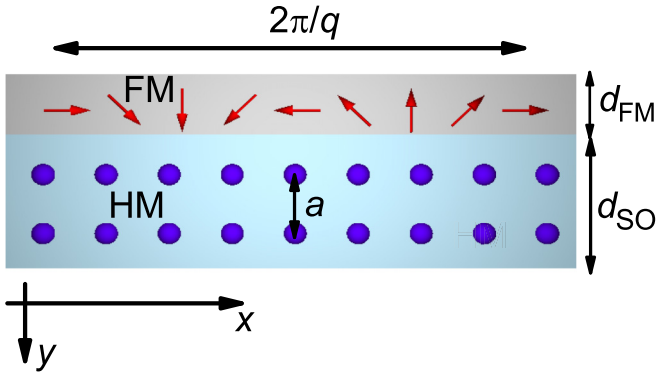


FIG. 1. Hybrid system with ferromagnetic (FM) and heavy-metal (HM) layers. Layers thicknesses are $d_{FM}$ and $d_{SO}$, respectively. Red arrows show magnetization of the FM layer. The magnetization forms the spiral state in the $(x, y)$ plane with spiral period being $2\pi/q$. Blue spheres are ions in the HM layer forming a lattice with interplane distance $a$.

$d_{SO}$. Electrons in the FM film are described by the $s$-$d$ model [30]. The single electron Hamiltonian reads

$$\hat{H}_{sd} = \frac{1}{2m}\hat{\mathbf{p}}^2 - J(\hat{\sigma}\mathbf{M}), \tag{1}$$

where $m$ is the effective mass of an electron. Here the effective mass is isotropic. However, in the general case the effective mass may be anisotropic (for example, when strain induces system anisotropy). $J$ is the exchange coupling constant describing the conductive electrons spin subbands splitting. This splitting is mostly due to interaction of conductive ($s$) electrons with localized ($d$) electrons forming magnetization of the FM film. $\mathbf{M}$ is the unit vector showing the direction of local magnetization. We assume that conductive electrons are free and can be described in the weak coupling model. The influence of the ionic potential is described using the effective electron mass $m$. In the HM layer an electron experiences a spin-orbit interaction and the Hamiltonian is given by

$$\hat{H}_{SO} = \frac{1}{2m}\hat{\mathbf{p}}^2 + \sum_i \lambda(|\mathbf{r} - \mathbf{r}_i|)(\hat{\sigma}\hat{\mathbf{l}}_i), \tag{2}$$

where the second term describes the spin-orbit interaction of an electron at each ion of HM ($y > 0$). Summation is performed over all ions with positions $\mathbf{r}_i$. The operator $\hat{\mathbf{l}}_i = [(\mathbf{r} - \mathbf{r}_i) \times \hat{\mathbf{p}}]$ is the electron orbital angular momentum with respect to the $i$th ion. $\lambda(|\mathbf{r} - \mathbf{r}_i|)$ is the SO interaction (SOI) spatial profile defined by the Coulomb potential produced by a single ion. $\lambda(|\mathbf{r}|)$ is a well localized function which is nonzero only in a small (compared to or less than an interatomic distance) region around an ion.

For simplicity we assume that ionic electrostatic potential in the HM film renormalizes the electron mass in the same way as in the FM layer. Therefore, the electron effective mass is the same in the whole space.

To calculate the total energy of electrons, we find electron wave functions and energies and sum over all states in the system. We consider the zero temperature limit. Therefore, all the states below the Fermi level $E_F$ are occupied and all the states above it are empty.

In the continuous limit the DMI at the interface is given by

$$W_{DMI} = D_x\left(M_x\frac{\partial M_y}{\partial x} - M_y\frac{\partial M_x}{\partial x}\right) + D_z\left(M_z\frac{\partial M_y}{\partial z} - M_y\frac{\partial M_z}{\partial z}\right), \tag{3}$$

where $D_x$ and $D_z$ are the DMI constants. If the system has in-plane anisotropy these constants can be different. We assume that magnetization is uniform across the magnetic film and the energy $W_{DMI}$ is the volume energy density (surface energy divided by the magnetic film thickness). Therefore, $D_{x,z}$ have the dimension of energy per unit area.

Energy contribution Eq. (3) leads to the formation of inhomogeneous helical magnetization distribution. To define the DMI strength we calculate the system energy for a magnetic spiral state described by

$$\mathbf{M} = (\cos(qx), \sin(qx), 0). \tag{4}$$

This is a magnetic spiral of the Néel type (common for systems with DMI). The spiral propagates along the FM/HM boundary with the rotation plane perpendicular to the interface. Note that the magnetic structure in Eq. (4) is considered for DMI calculations only. The real magnetic structure of the film should be calculated by taking into account all energy contributions such as magnetic anisotropy, dipole-dipole interaction, exchange interaction, and DMI.

Substituting Eq. (4) into Eq. (3) one finds that DMI is linear in $q$, $W_{DMI} = qD_x$. Note that beside the DMI energy there is also the exchange interaction between localized magnetic moments in the FM film (not taken into account in the model since it does not influence the DMI). This interaction is quadratic in $q$ and stabilizes magnetic spiral with a certain wavelength.

Using the above Hamiltonian [Eqs. (1) and (2)] we find the electron energy as a function of $q$ and check if it has a linear in $q$ terms. First, we find the electron wave functions for the system without the spin-orbit interaction. The nonperturbed Hamiltonian has the form

$$\hat{H}^{(0)} = \begin{cases} \dfrac{\hat{\mathbf{p}}^2}{2m} - J[\sigma_x\cos(qx) + \sigma_y\sin(qx)], & y < 0, \\ \dfrac{\hat{\mathbf{p}}^2}{2m}, & y > 0. \end{cases} \tag{5}$$

Next, we calculate the SO interaction energy using the first order perturbation theory where perturbation reads

$$\hat{H}^{(1)} = \begin{cases} 0, & y < 0, \\ \displaystyle\sum_i \lambda(|\mathbf{r} - \mathbf{r}_i|)(\hat{\sigma}\hat{\mathbf{l}}_i), & y > 0. \end{cases} \tag{6}$$

## III. DMI CALCULATIONS

### A. Electron wave functions

First, we consider the nonperturbed Hamiltonian in Eq. (5). We use the adiabatic approximation where electron spin follows the local magnetization direction in the FM. The small parameter in this case is $\beta = \hbar^2 q k_x/(mJ) \ll 1$. For small $q$ limit (used to find linear in $q$ energy correction), the above inequality is always valid. Additionally, in metallic ferromagnets the exchange interaction is usually strong supporting

our assumption. The quasiadiabatic (of order of $\sim\beta^1$, and of higher orders) corrections can be neglected when calculating electron wave functions and unperturbed energy, see Appendix A. In Ref. [23] the exchange interaction was treated as a perturbation (which is not a good approximation for a metallic ferromagnet). Here we consider the opposite limit. In Ref. [24] the exchange ($sd$) field was treated as perturbation, however this field was linearly changing in space. Therefore, the DMI in Ref. [24] appears in the second order perturbation theory (exchange variation + SO interaction). In our work we find the DMI as a first order perturbation correction due to the SOI. At that, the exchange interaction is included in the zero order Hamiltonian.

The single electron wave function for $y<0$ (we indicate this region with the index 1) has the form

$$\psi_{\mathbf{k}}^{1\pm}=\frac{1}{\sqrt{2}}e^{ik_x x+ik_z z}e^{ik_{1y}^{\pm}y}\begin{pmatrix}\pm e^{-iqx/2}\\ e^{iqx/2}\end{pmatrix}. \tag{7}$$

The sign + (−) stands for electron spin co-directed (counter-directed) with local magnetization **M**. Electron energy is given by

$$E^{\pm}_{k_x,k_{1y},k_z}=\frac{\hbar^2}{2m}\mathbf{k}^2\mp J. \tag{8}$$

The wave function in Eq. (7) has different $x$ quasimomentum for up and down spinor components. To satisfy the boundary conditions we compose the wave function in the HM layer ($y>0$, indicated by the index 2) of two plain waves $\exp(i\mathbf{kr})$ with different $x$ momentums:

$$\psi_{\mathbf{k}}^{2\pm}=\frac{1}{\sqrt{2}}e^{ik_z z}\begin{pmatrix}\pm e^{ik_{2y}^{+}y+i(k_x-q/2)x}\\ e^{ik_{2y}^{-}y+i(k_x+q/2)x}\end{pmatrix}. \tag{9}$$

Note that energies of spin-up and spin-down states are the same:

$$\begin{aligned}E_{k_x,k_{2y}^{+},k_z}&=\frac{\hbar^2}{2m}\left[k_z^2+k_{2y}^{+2}+(k_x-q/2)^2\right]\\&=\frac{\hbar^2}{2m}\left[k_z^2+k_{2y}^{-2}+(k_x+q/2)^2\right].\end{aligned} \tag{10}$$

This gives the relation

$$k_{2y}^{+2}=k_{2y}^{-2}-2qk_x. \tag{11}$$

Note that due to the boundary conditions $k_x$ and $k_z$ should be the same for the wave function in both layers. The components along the $y$ direction are related as follows:

$$(k_{1y}^{\pm})^2=k_{2y}^{\pm 2}\mp qk_x\pm J. \tag{12}$$

Quadratic in $q$ term is neglected within our approximation.

The full wave function consists of several plain waves in each layer:

$$\begin{aligned}\Psi_{k_x,k_{1y}^{+},k_z}&=\frac{1}{N}e^{i(k_z z+k_x x)}\left\{\begin{pmatrix}(B_{\rightarrow}^{+}-B_{\rightarrow}^{-})e^{ik_{2y}^{+}y-i\frac{qx}{2}}\\ (B_{\rightarrow}^{+}+B_{\rightarrow}^{-})e^{ik_{2y}^{-}y+i\frac{qx}{2}}\end{pmatrix}\right.\\&\left.+\begin{pmatrix}(B_{\leftarrow}^{+}-B_{\leftarrow}^{-})e^{-ik_{2y}^{+}y-i\frac{qx}{2}}\\ (B_{\leftarrow}^{+}+B_{\leftarrow}^{-})e^{-ik_{2y}^{-}y+i\frac{qx}{2}}\end{pmatrix}\right\},\quad y>0,\\ \Psi_{k_x,k_{1y}^{+},k_z}&=\frac{1}{N}e^{i(k_z z+k_x x)}\\&\times\left\{A_{\rightarrow}^{+}e^{ik_{1y}^{+}y}\begin{pmatrix}e^{-i\frac{qx}{2}}\\ e^{i\frac{qx}{2}}\end{pmatrix}+A_{\rightarrow}^{-}e^{ik_{1y}^{-}y}\begin{pmatrix}-e^{-i\frac{qx}{2}}\\ e^{i\frac{qx}{2}}\end{pmatrix}\right.\\&\left.+A_{\leftarrow}^{+}e^{-ik_{1y}^{+}y}\begin{pmatrix}e^{-i\frac{qx}{2}}\\ e^{i\frac{qx}{2}}\end{pmatrix}+A_{\leftarrow}^{-}e^{-ik_{1y}^{-}y}\begin{pmatrix}-e^{-i\frac{qx}{2}}\\ e^{i\frac{qx}{2}}\end{pmatrix}\right\},\\ &y<0.\end{aligned} \tag{13}$$

Using boundary conditions at $y=-d_{\mathrm{FM}}$, $y=0$, and $y=d_{\mathrm{SO}}$ we obtain a system of eight linear equations for eight unknown coefficients $A_{\rightarrow}^{\pm}$, $A_{\leftarrow}^{\pm}$, $B_{\rightarrow}^{\pm}$, and $B_{\leftarrow}^{\pm}$. Using the condition Det = 0 (where Det is the system determinant) we find the energy levels and $y$ quasimomentums. We find zeros of the determinant numerically. Note that there is no quasimomentum quantization along $x$ and $z$ directions, but there is a quantization along the $y$ direction. Finally, we find the wave functions for given $k_x$, $k_z$, and $k_{1y}^{+}$. We chose these quantum numbers to enumerate the electron states. These quantum numbers are real. Note that there will be states with spin mostly co-directed with the FM magnetization and states with spins counter-directed to magnetization. These states have different quasimomentums $k_{1y}$. Therefore we do not need to introduce an additional quantum number responsible for a spin state of a particle. The normalization factor $1/N$ of electron wave function is discussed in Appendix A.

### B. Properties of SO interaction

Consider the average energy of the SO *interaction* between a single electron with a single ion in the HM layer. The energy correction is given by

$$W_{\mathrm{SO}}^{(i)}=\langle\Psi|\lambda(|\mathbf{r}|)(\hat{\sigma}\cdot[\mathbf{r}\times\mathbf{p}])|\Psi\rangle. \tag{14}$$

The superscript $i$ stands for the $i$th HM ion. As an example, consider a single term in this expression $\langle\Psi|\lambda(|\mathbf{r}|)\sigma_x y p_z|\Psi\rangle$. This contribution is an odd (linear) function of $k_z$ since the wave functions are the harmonic plain waves in the $z$ direction. Taking into account the fact that electron spectrum is an even function of $k_z$ the contribution of this term into the total SO energy is zero after averaging over all electron states. Therefore, all terms with $p_z$ do not contribute to the SO interaction energy. Now consider the term $\langle\Psi|\lambda(|\mathbf{r}|)\sigma_x z p_y|\Psi\rangle$. From Eq. (13) one can see that the electron spin and mass densities do not depend on the $z$ coordinate. Therefore, this matrix element is also zero after integrating over coordinates. So, elements with $z$ do not contribute to the SOI energy. Now consider the term of the form $\langle\Psi|\lambda(|\mathbf{r}|)\sigma_z x p_y|\Psi\rangle$. One can show that $z$ component of the electron spin does not depend on $x$. Therefore, this term also cancels out. The only term that contribute to the SO energy has the form

$$W_{\mathrm{SO}}^{(i)}=\langle\Psi|\lambda(|\mathbf{r}|)\sigma_z y p_x|\Psi\rangle. \tag{15}$$

First consider one part of the wave function traveling outward the interface. For high enough energies the wavenumbers $k_{2y}^{+}$ and $k_{2y}^{-}$ are real. Such a wave function has the form

$$\Psi_{\rightarrow}^{+}=\frac{e^{i(k_z z+k_x x)}}{\sqrt{2}}\begin{pmatrix}(B_{\rightarrow}^{+}-B_{\rightarrow}^{+})e^{ik_{2y}^{+}y-i\frac{qx}{2}}\\ (B_{\rightarrow}^{+}+B_{\rightarrow}^{+})e^{ik_{2y}^{-}y+i\frac{qx}{2}}\end{pmatrix}. \tag{16}$$

One can see that the $z$ component of the spin is independent of $y$. Therefore, Eq. (16) is an odd function of $y$ and vanishes after averaging over coordinates. A similar situation is for the wave purely traveling toward the interface. Finally, only the interference of waves traveling backward and forward contribute to the SOI. This interference is the origin of oscillations of electron magnetic moment which contribute to the SOI.

If the wave has an imaginary quasimomentum it also contributes to the SOI, since the $z$ component of the electron spin varies exponentially in this case.

### C. SOI energy

For the states with real $k_{2y}^{\pm}$ the expression for the energy of SO interaction between a single electron and a single ion at the position $y_i$ is the following:

$$W_{\mathrm{SO}}^{(i)}(k_x, k_{1y}^{+}, k_z) = -2I\mathrm{Re}\big(ik_{2y}^{+}(k_x - q/2)(B_{\rightarrow}^{+} - B_{\rightarrow}^{-})^{*}(B_{\leftarrow}^{+} - B_{\leftarrow}^{-})e^{-2ik_{2y}^{+}y_i} - ik_{2y}^{-}(k_x + q/2)(B_{\rightarrow}^{+} + B_{\rightarrow}^{-})^{*}(B_{\leftarrow}^{+} + B_{\leftarrow}^{-})e^{-2ik_{2y}^{-}y_i}\big), \tag{17}$$

where $I$ is given by

$$I = \frac{2\hbar}{N}\int d^3 r y^2 \lambda(|\mathbf{r}|). \tag{18}$$

In the above expressions we use the fact that $\lambda$ is nonzero in the small region around $|\mathbf{r} - \mathbf{r}_i| = 0$. In this region we write the exponents $e^{2ik_{2y}^{+}(y+y_i)} \approx e^{2ik_{2y}^{+}y_i}(1 + 2ik_{2y}^{+}y)$. The first term is even in $y$ and does not contribute to the SOI. Only the term linear in $y$ gives the nonzero matrix element. The SOI energy correction does not depend on $k_z$. Note that $I$ is inversely proportional to the system volume. However, the number of ions is proportional to the system volume. Therefore the DMI coefficient contains only the ion density which is finite.

It is important that the matrix element of SOI does not depend on the position of the HM ion in the film plane (on $x$ and $z$ coordinates). Therefore, the total DMI does not depend on the distance between the HM ions in the film plane. Only the distance between ions in the $y$ direction is important. As a result only the strain along the $y$ direction influences the DMI.

Results for states with imaginary quasimomentums are given in Appendix B.

Now we average the energy correction in Eq. (17) over all electron states and all ions in the HM layer:

$$W_{\mathrm{SO}}^{\mathrm{tot}} = \frac{S}{4\pi^2}\sum_{y_i}\sum_{k_{1y}^{+}}\int dk_x \int dk_z W_{\mathrm{SO}}^{i}(k_x, k_{1y}^{+}) = \frac{S}{2\pi^2}\sum_{y_i}\sum_{k_{1y}^{+}}\int_{-k_{\mathrm{F}}}^{k_{\mathrm{F}}} dk_x \times \sqrt{\tilde{E}_{\mathrm{F}} - k_x^2 - k_{1y}^{+2} - 2\tilde{J}}\, W_{\mathrm{SO}}^{i}(k_x, k_{1y}^{+}). \tag{19}$$

Here we introduce normalized energies $\tilde{E}_{\mathrm{F}} = E_{\mathrm{F}}/(\hbar^2/2m)$ and $\tilde{J} = J/(\hbar^2/2m)$. The quantity $S$ is the interface area and $k_{\mathrm{F}}$ is the Fermi momentum.

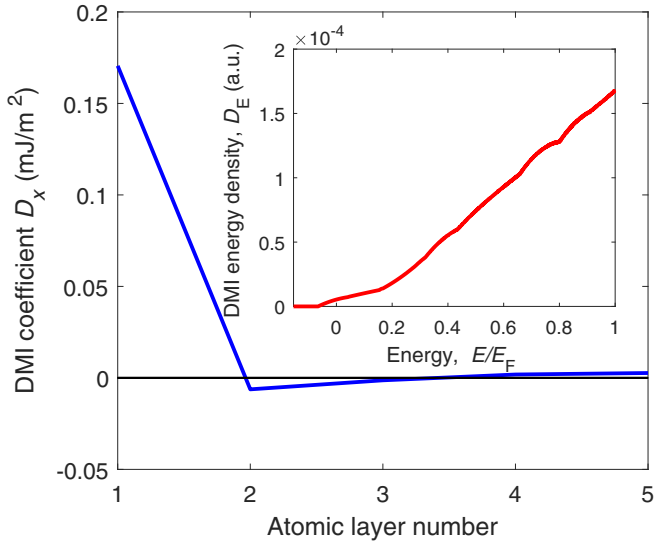


FIG. 2. Contribution of each layer of HM to the DMI coefficient $D_x$. HM and FM layer thickness is fixed, $d_{\mathrm{SO}} = 5$ and $d_{\mathrm{FM}} = 3$ atomic layers. Other parameters are discussed in the text. Inset shows the energy density of DMI, $D_E$ (see text for definition).

### D. Relation between the DMI coefficient and the SO energy

As we mentioned above, the DMI energy in the system with the spiral magnetization is defined by $W_{\mathrm{DMI}} = qD_x$. The SOI energy is the only contribution which has a linear in $q$ part. Thus, we can write

$$D_x = \frac{1}{d_{\mathrm{FM}}S}\frac{\partial W_{\mathrm{SO}}^{\mathrm{tot}}}{\partial q}\bigg|_{q\to 0}. \tag{20}$$

Similarly one can calculate the DMI constant $D_z$. In this case one needs to consider a magnetic spiral propagating along the $z$ direction.

### E. Contribution to the DMI from different HM ion layers

Figure 2 shows how each layer in the HM film contributes to the DMI coefficient. The following parameters are used: the thickness of the HM layer is $d_{\mathrm{SO}} = 5$ atomic planes; the FM layer thickness is $d_{\mathrm{FM}} = 3$ atomic layers; electrons concentration is $n_{\mathrm{el}} = 0.5$ electrons per atom which is the characteristic carrier concentration in Co [31]; and exchange interaction is of order of 1 eV [32] which is about $0.12E_{\mathrm{F}}$ [33] ($E_{\mathrm{F}} = 8.5$ eV).

The strength of the SO interaction is defined by the constant $I$. It has the dimension of energy $\times$ length$^2$. We introduce the quantity with the dimension of energy as follows. Parameter $I$ describes the interaction of an electron with a single SO ion. At that the electron is smeared over the whole sample. So, we multiply $I$ by the number of ions in the system to avoid the factor $1/V$ ($V$ is the system volume). Also to get the energy units we multiply $I$ by the quasimomentum square. The DMI matrix element in Eq. (17) is linear in $q$ (for small $q$). So, $q$ would be one of two characteristic quasimomenta. The second one is the Fermi momentum. Finally, we introduce a characteristic SO energy per unit cell contributing to the DMI interaction as follows $IN_{\mathrm{sites}}qk_{\mathrm{F}}$. For estimates we

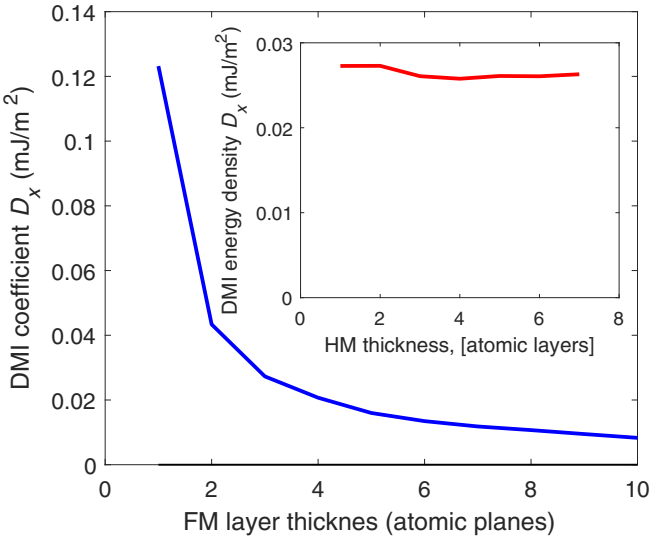


FIG. 3. Dependence of the DMI coefficient $D_x$ on FM layer thickness. Inset shows the DMI coefficient $D_x$ as a function of HM layer thickness.

use the value $0.01E_F$ for this energy. Note that DMI linearly scales with $I$. Therefore, this parameter does not influence any dependencies shown below.

Figure 2 shows that the DMI interaction appears mostly in the first HM layer. This is in agreement with *ab initio* simulations [34]. Also this follows from the fact that the matrix element in Eq. (17) is the fast oscillating function of $y$ coordinate. These oscillations are defined by the wave vector of electrons. Electrons with different quasimomentum approach a particular HM ion with different phase. This phase is the same only for ions in the close vicinity to the interface. For ions away from the interface the wave functions of various states are dephased leading to cancellation of contributions from different electrons.

The inset in Fig. 2 shows how electrons with different energies contribute to the DMI. This quantity can be expressed as $D_E(E)dE \sim \sum_{y_i} \int dk_x \int dk_z \sum_{k_{1y}^+, |E_{k_x,k_{1y},k_z} - E| < dE/2} W_{SO}^i$. One can see that all states in the conduction band contribute, however the states with higher energy contribute more. This is because the high energy electrons have higher orbital momentum and therefore show stronger SOI. Peculiarities in the curve are related to energy quantization, which is important due to small thickness of the layers.

### F. DMI dependence on the layers thickness

The DMI coefficient decreases with $d_{FM}$ since this is a surface effect and should decrease as $1/d_{FM}$ (see Fig. 3). The inset in Fig. 3 shows the dependence on the HM layer. One can see that there is practically no dependence on the HM layer since only the first layer contributes.

## IV. DMI DEPENDENCE ON STRAIN

The strain in the film FM/HM film can be created in different ways. One can use a ferroelectric crystal as a substrate for FM/HM film. Applying voltage to such a crystal induces strain in it. This strain is transferred into the magnetic multilayer film. For example, using PMN-PT with orientation (001) as a substrate allows us to create isotropic in-plane strain in the HM/FM system. A different cut [(110) for example] of PMN-PT can be used to create an anisotropic in-plane strain. Even without the FE crystal the strain can be induced with bending the sample. In this case the strain is anisotropic in-plane. Note that due to the Poisson law the in-plane strain should inevitably induce the out-of-plane one. At that the volume of the FM/HM film is not conserved. Typical strain that can be achieved is usually less than 1%.

We mention that in this work we do not consider the share strains and only the diagonal components of the strain are nonzero.

### A. Mechanisms of strain dependence

There are several contributions to the strain dependence of DMI constant.

(1) The effective mass of the electron depends on the strain $m = m(\varepsilon)$. One can expect that it grows with positive strain. Increasing the distance between the ions leads to stronger localization of electrons and increases the effective mass. So, we assume that $m_{x,y,z} = m_0(1 + m_1\varepsilon_{xx,yy,zz})$. If we apply an isotropic in-plane strain to a thin film we have $\varepsilon_{xx} = \varepsilon_{zz}$, $\varepsilon_{yy} = -2\nu\varepsilon_{xx}/(1-\nu)$. Here $\nu$ is the Poisson ratio which is of order of 1/3 for metals [35]. Finally, the isotropic in-plane strain leads to mass anisotropy. Positive in-plane strain increases the in-plane effective mass and decreases the mass in the out-of-plane direction.

(2) The exchange constant $J$ also changes due to a strain. $J$ defines the effective magnetic field acting on the spin of conduction electrons. The field is produced by the localized magnetic moments. In a stretched FM film the density of magnetic ions decreases leading to a smaller effective field. The coupling constant $J$ should scale with volume of the FM layer as $J = J_0V_0/V$, where $J_0$ and $V_0$ are the exchange constant and the volume in the absence of strain. For isotropic in-plane strain one has $J \approx J_0(1 + \varepsilon_{yy})$. Similarly the SO interaction constant $I$ scales with the strain as $I \approx I_0(1 + \varepsilon_{yy})$, where $I_0$ is the SO constant for zero strain.

(3) Strain changes the thickness of the magnetic layers. This rearranges the locations of the SO ions $\mathbf{r}_i$. The lattice constant (distance between ions) changes according to the applied strain. As we mentioned above the in-plane position of the HM ions is not important. Positive isotropic in-plane strain increases the in-plane lattice constant and decreases the out-of-plane constant $a_{x,y,z} = a_0(1 + \varepsilon_{xx,yy,zz})$ ($a_0$ is the lattice constant for the unstrained sample, we consider the cubic lattice here, but our results can be generalized to different lattices). Since the ion positions directly enter the Hamiltonian we do not need to introduce any phenomenological constants (as in the case of effective mass variation). Lattice constant variation influences the SO matrix elements since the electrons approach the ions with different phases compared to the unstrained sample. Variation of the film thickness also modifies the quantization conditions leading to reshaping of electron wave functions and to changing of eigenenergies.

Below is shown that this last contribution is the most important one and can induce a large variation of the DMI

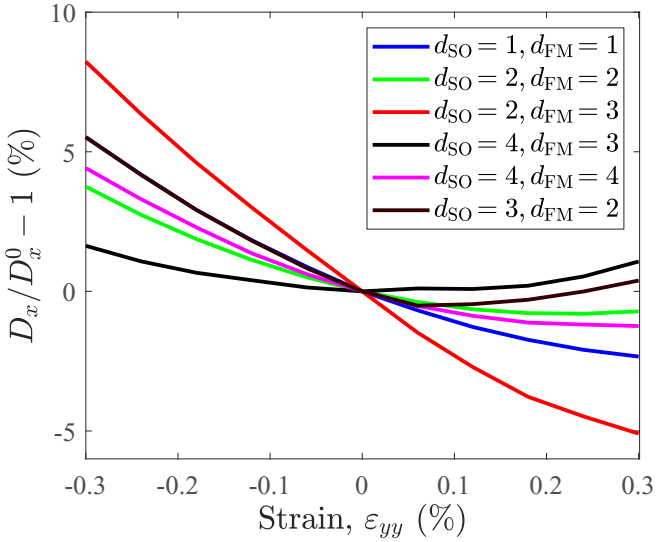


FIG. 4. Relative variation of the DMI coefficient as a function of applied strain $\varepsilon_{yy}$. $D_x^0$ is the DMI coefficient at zero strain. Electron density $n_{el} = 0.5$ electron per site, exchange constant $J_0 = 0.2E_F$, and SOI constant $I$ are the same for all curves. Thickness of FM and HM layers (measured in atomic planes) is different.

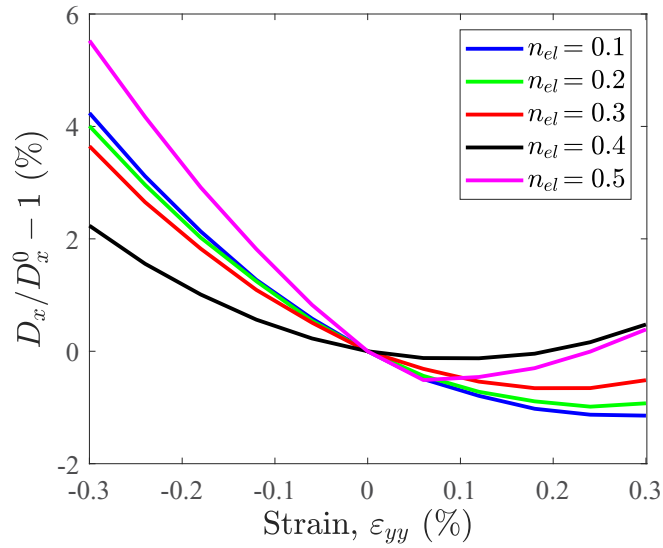


FIG. 5. Relative variation of the DMI coefficient as a function of applied strain $\varepsilon_{yy}$. $D_x^0$ is the DMI coefficient at zero strain. Thickness $d_{FM} = 2$ atomic layers, $d_{SO} = 3$ atomic layers, and exchange constant $J_0 = 0.2E_F$ are the same for all curves. The electron density $n_{el}$ varies.

constant. Variation of the effective mass and constants $I$ and $J$ should be of order of the applied strain and should induce the corresponding DMI variation (of order of a few %). Variation of ions position affects the electron phase. Since the electron wave functions oscillates in space quickly (at Fermi wavelength) even small displacement of the ions leads to big variation of the phase of SO matrix element.

### B. Strain dependence of the DMI constant

Figure 4 shows how the DMI coefficient depends on strain for systems with different layer thickness. A relative variation of $D_x$ is shown. The applied strain is isotropic in the film plane ($\varepsilon_{xx} = \varepsilon_{zz}$). The isotropic in-plane strain induces the out-of-plane strain $\varepsilon_{yy}$ due to the Poisson law. As we mention before, the matrix elements of the SOI do not depend on the in-plane positions of the HM ions meaning that in-plane strain itself does not affect the DMI. Therefore, we plot all the curves here as a function of $\varepsilon_{yy}$.

The Fermi energy is chosen such that there is 0.5 electrons per site. The exchange coupling constant $J_0 \approx 0.15E_F$. Value of $I_0$ is not important for relative variation of the DMI constant. Several curves are shown for different FM and HM layer thickness.

The DMI coefficient depends on strain. The strain of order of 0.3% induces a variation of the DMI coefficient of the order of 6%. The DMI coefficient is a nonlinear function of strain and it decreases with strain. Also one can see that the dependence $D_x(\varepsilon_{yy})$ varies with FM and HM layer thickness. There is an optimum thickness (around 2 monolayers of FM and 2 monolayers of HM) of the system giving the highest slope. At smaller and larger thickness the DMI variation becomes weaker. Also at large thickness the DMI constant variation becomes strongly nonlinear and has a minimum at small strain.

Figure 5 shows the dependence of the DMI coefficient on strain for various electron density in the system. The thickness of FM and HM metals is fixed, $d_{FM} = 2$ atomic planes and $d_{SO} = 3$ atomic layers. The exchange coupling constant is fixed, $J_0 = 0.2E_F$. One can see that the relative variation of the DMI coefficient is almost independent of the electron concentration. It is of order of 5% for all concentrations. However, the absolute value of DMI coefficient increases with electron concentration.

One can see that the strain dependence of the DMI is not monotonic. $D_x$ decays at negative strain, but starts to increase at positive $\varepsilon_{yy}$. This is related to the fact that DMI is induced by conduction electrons. The phase of the electronic wave function oscillates in space quickly leading to oscillating interaction. The situation is similar to Ruderman-Kittel-Kasuya-Yosida (RKKY) interaction which oscillates as $\cos(k_F a)$. The expression obtained by Levy and Fert for the DMI between two FM ions also contains a similar factor (see Eq. (5) in Ref. [23]). So, the nonmonotonic behavior of the DMI with strain (interatomic distance) is due to the oscillating nature of the interaction.

Strain sensitivity of the DMI coefficient also depends on the exchange coupling constant, see Fig. 6. One can see that $D_x$ variation increases with exchange constant $J$, however this increase is not very big, 3%–6%.

Finally, Fig. 7 shows the strain dependence of the DMI coefficient for various initially strained states. We assume that the initial state is strained already and apply additional deformations to the system. The initial strain is denoted as $\varepsilon_{yy}^0$. It can appear due to growth condition, lattice mismatch, and other factors. Usually, the initial strain defines the equilibrium lattice constant. Figure 7 shows that for system with the lattice constant 3% smaller than the initial one we a have large variation of DMI coefficient reaching ±40% under strain of 0.3%. The parameter $D_x$ changes twice when changing strain

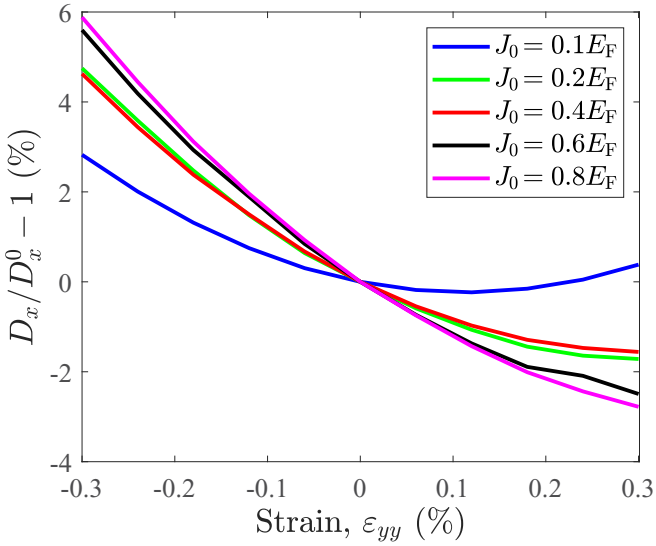


FIG. 6. Relative variation of the DMI coefficient as a function of applied strain $\varepsilon_{yy}$. $D_x^0$ is the DMI coefficient at zero strain. Electron density $n_{el} = 0.5$ electron per site, thickness $d_{FM} = 3$ and $d_{SO} = 2$ atomic planes, and SOI constant $I_0$ are the same for all curves. The exchange coupling constant $J_0$ varies.

from $-0.3\%$ to $+0.3\%$ strain. This change is comparable with experimental data.

### C. Strain induced DMI anisotropy

Above we discuss the isotropic ($\varepsilon_{xx} = \varepsilon_{zz}$) strain in the ($x$, $z$) plane. Here we consider the anisotropic one. We compare two limits when $yy$ component of the strain is produced by the uniaxial deformation along either $x$ axis or $z$ axis. Both types of deformation lead to the same $\varepsilon_{yy}$. The only difference

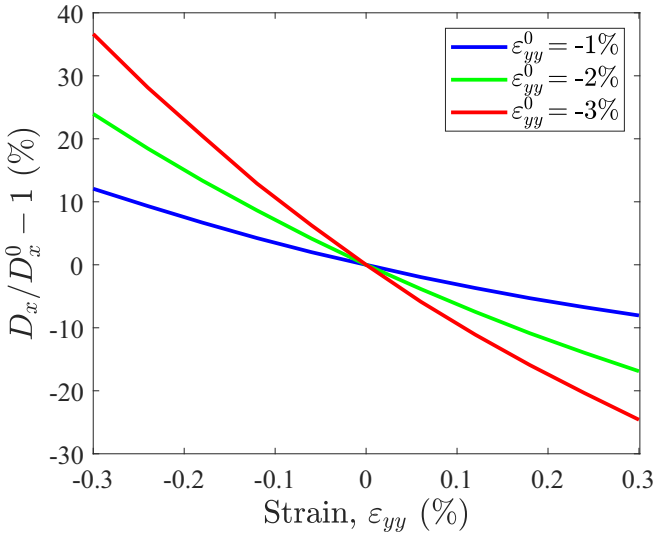


FIG. 7. Relative variation of the DMI coefficient as a function of applied strain $\varepsilon_{yy}$. $D_x^0$ is the DMI coefficient at zero strain. Electron density $n_{el} = 0.5$ electron per site, thickness $d_{FM} = 3$ atomic planes and $d_{SO} = 2$, $J_0 = 0.2E_F$, and SOI constant $I_0$ are the same for all curves. The initial system strain $\varepsilon_{yy}^0$ varies.

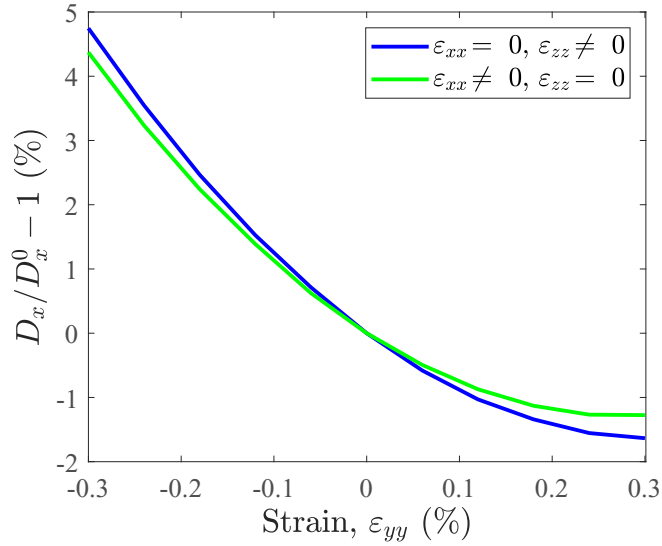


FIG. 8. Relative variation of the DMI coefficient as a function of applied strain $\varepsilon_{yy}$. $D_x^0$ is the DMI coefficient at zero strain. Electron density $n_{el} = 0.5$ electron per site, thickness $d_{FM} = 1$ and $d_{SO} = 2$ atomic planes, $J_0 = 0.2E_F$, and SOI constant $I_0$ are the same for all curves. Effective mass is anisotropic due to anisotropic strain in the ($x$, $z$) plane. Orientation of the uniaxial in-plane strain is shown in the legend.

between these two limits is that the effective mass along $x$ and $z$ axes is different. At that the magnetic spiral propagates along $x$ axis in both cases. When we deform the system uniaxially along the $x$ axis the mass along the $z$ axes does not change and vice versa. Since positions in the ($x$, $z$) plane of the HM ions are not important for the SOI matrix elements, the anisotropy of the effective mass is the only mechanism contributing to DMI anisotropy in our model. Figure 8 shows the relative variations of DMI coefficient for strains applied along $x$ and $z$ directions. Indeed, one can see that the DMI coefficient is anisotropic but this effect is weak.

### D. Different contributions to the DMI coefficient

There are several mechanisms influencing the DMI under applied strain: (1) varying distance between ions in HM layer, (2) varying effective electron mass, (3) varying effective exchange constant due to volume variation, etc. To define the main factor for strain-dependent DMI we remove some of the mechanisms and compare the DMI sensitivity to strain. Figure 9 shows the dependence of $D_x$ on $\varepsilon_{yy}$ for different cases when all mechanisms work, when mechanism 2 is suppressed, or when mechanism 3 is switched off. As one can see all mechanisms contribute to $D_x(\varepsilon_{yy})$ behavior. However, the influence of mechanisms 2 and 3 is not very pronounced. Therefore, the distance variation between HM ions is the main mechanism of DMI sensitivity to the strain.

## V. DISCUSSION

### A. Comparison to experiment

Recent experiment in Ref. [22] shows the dependence of the DMI on strain. The model considered in the current paper

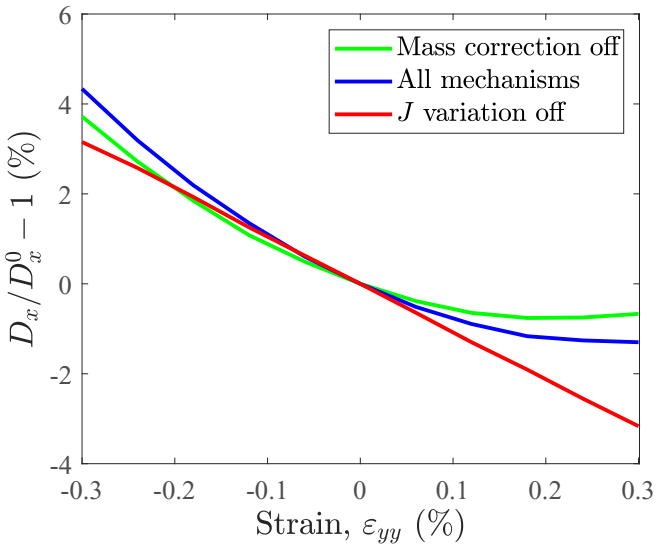


FIG. 9. Relative variation of the DMI coefficient as a function of applied strain $\varepsilon_{yy}$. $D_x^0$ is the DMI coefficient at zero strain. Electron density $n_{\rm el} = 0.5$ electron per site, thickness $d_{\rm FM} = 3$ atomic planes and $d_{\rm SO} = 2$, $J_0 = 0.2E_{\rm F}$, and SOI constant $I_0$ are the same for all curves. No initial strain is applied. Various mechanisms of the DMI strain dependence are removed.

is a toy model that cannot describe the experimental data on a quantitative level. We consider an ideal crystal structure with an ideal lattice match. In the experiment however, the magnetron sputtering was used to prepare the samples. This means that the films consist of crystallites with different orientation of lattice vectors. The interface also is not ideal when this method is used. It is rough and intermixed. The lattice constants of both Co and Pt are defined by the tantalum underlayer and the embedded strain (used in our modeling) is not known. Nevertheless, we can check if our model can reproduce some prominent features of the experiment: (1) relative DMI variation larger than the strain (relative lattice constant change); (2) anisotropy of DMI induced by the anisotropic strain; and (3) change of the DMI sign due to the strain.

The model discussed in the present work can produce large variations of DMI coefficient. The relative change of the DMI is much larger than the relative variation of the interatomic distance. This is in agreement with experimental data of Ref. [22]. In Ref. [22] the DMI coefficient grows with positive $\varepsilon_{xx}$ deformations. We plot the DMI coefficient as a function of $\varepsilon_{yy}$. As we discussed above, $\varepsilon_{xx}$ and $\varepsilon_{yy}$ are related through the Poisson law. At that, they have different sign. So, positive $\varepsilon_{xx}$ means negative $\varepsilon_{yy}$ and decreasing of the DMI with $\varepsilon_{yy}$ is the same as increasing DMI with $\varepsilon_{xx}$. So, the trend observed in our simulations is the same as in the experiments in Ref. [22].

Another experimental finding is that DMI shows a strong anisotropy due to anisotropic in-plane strain. We also reproduce the anisotropy of DMI. However, the anisotropy in our simulations is smaller than in experiment.

The third main observation in Ref. [22] is the change of the DMI sign with strain. We cannot reproduce this effect using our model. It is possible that there are other mechanisms of the DMI (such as Rashba effect at FM/HM interface). This additional contribution may have the opposite sign. Competition of different mechanisms can lead to sign change. Doing more rigorous simulations by taking into account the band structure can probably reproduce the whole spectrum of observed phenomena.

### B. Other possibilities for DMI strain dependence

(1) There are other mechanisms of the DMI interaction in the bilayer system. For example, the embedded electric field at the interface between the FM and HM can induce the Rashba spin-orbit interaction leading to the DMI. The sensitivity of this contribution to strain effects is an open question and will be considered in a forthcoming work.

(2) We use the zero-order perturbation theory in the quasiadiabatic approximation in the FM metal and the first order perturbation theory in SO interaction. The first approximation is justified because we study the limit of small $q$. However, the second approximation can be violated in real materials. Therefore, it is interesting to study the limit of strong SOI.

(3) We never discuss the real band structure of the FM and HM. We consider the problem within the effective mass approximation assuming that there is no internal structure of the wave function at HM ions. This approximation is often used for $s$ electrons. We use it for all conductive electrons in the system. In HMs $p$ and $d$ electrons are very important. They have nonzero orbital moment with respect to ions and therefore demonstrate strong SOI. It would be interesting to study how strain affects SOI of electrons with a more complicated wave function (such as $p$ or $d$ electrons). This can be done using *ab initio* simulations [34].

## VI. CONCLUSION

We studied the dependence of the DMI in the bilayer system FM/HM on the mechanical strain applied to it. To calculate the DMI coefficient we took into account only the mechanism related to the SOI in the bulk of the HM metal and neglected the Rashba interaction at the HM/FM interface due to embedded surface field. We showed that the DMI constant varies with strain (isotropic in the film plane). While the deformations can be quite small (on the order of 0.3%) the DMI variation can be as high as 70%. This is in agreement with recent experimental data on the strain-dependent DMI. The strain dependence of the DMI is mostly related to the variation of the distance between the atomic planes in HM layer and variation of boundary conditions for the wave function. So, the deformations along the axis perpendicular to the film plane are important. At that the deformations in the plane of the film do not contribute to the DMI variation. The anisotropy of DMI interaction may appear if the strain is anisotropic in the plane of the FM/HM bilayer. In our model the anisotropy appears due to the anisotropy of effective mass in the film plane. Sensitivity of the DMI constant to the strain depends on the system parameters.

## ACKNOWLEDGMENTS

This research was supported by NSF under Cooperative Agreement Award No. EEC-1160504. O.G.U. was supported by the Russian Science Foundation (Grant 18-72-10026).

## APPENDIX A: WAVE FUNCTION NORMALIZATION FOR THIN FILM SYSTEM

The normalizing constant $N$ is given by

$$1/N^2 = N_1 + N_2, \tag{A1}$$

where $N_1$ is defined by

$$\begin{aligned} N_1 &= 2d_{\mathrm{FM}}(|A^+_{\rightarrow}|^2 + |A^+_{\leftarrow}|^2) + \frac{|A^-_{\rightarrow}|^2}{\kappa^-_{1y}}(e^{2\kappa^-_{1y}d_{\mathrm{FM}}} - 1) \\ &+ \frac{|A^-_{\leftarrow}|^2}{\kappa^-_{1y}}(1 - e^{-2\kappa^-_{1y}d_{\mathrm{FM}}}) + 2\mathrm{Re}\left(\frac{A^{+*}_{\rightarrow}A^+_{\leftarrow}}{ik^+_{1y}}(e^{2ik^+_{1y}d_{\mathrm{FM}}} - 1)\right) \\ &+ 4d_{\mathrm{FM}}\mathrm{Re}(A^{-*}_{\rightarrow}A^-_{\leftarrow}). \end{aligned} \tag{A2}$$

for imaginary $k^-_{1y}$ ($\kappa^-_{1y} = |k^-_{1y}|$). For real $k^-_{1y}$ we have

$$\begin{aligned} N_1 &= 2d_{\mathrm{FM}}(|A^+_{\rightarrow}|^2 + |A^+_{\leftarrow}|^2 + |A^-_{\rightarrow}|^2 + |A^-_{\leftarrow}|^2) \\ &+2\mathrm{Re}\left(\frac{A^{+*}_{\rightarrow}A^+_{\leftarrow}}{ik^+_{1y}}(e^{2ik^+_{1y}d_{\mathrm{FM}}} - 1)\right) \\ &+2\mathrm{Re}\left(\frac{A^{-*}_{\rightarrow}A^-_{\leftarrow}}{ik^-_{1y}}(e^{2ik^-_{1y}d_{\mathrm{FM}}} - 1)\right). \end{aligned} \tag{A3}$$

The second contribution to $N$ is defined by

$$\begin{aligned} N_2 &= 2d_{\mathrm{SO}}(|B^+_{\rightarrow}|^2 + |B^+_{\leftarrow}|^2 + |B^-_{\rightarrow}|^2 + |B^-_{\leftarrow}|^2) \\ &+\mathrm{Re}\left(\frac{(B^+_{\rightarrow} - B^-_{\rightarrow})^*(B^+_{\leftarrow} - B^-_{\leftarrow})}{-ik^+_{2y}}(e^{-2ik^+_{2y}d_{\mathrm{SO}}} - 1)\right) \\ &+\mathrm{Re}\left(\frac{(B^+_{\rightarrow} + B^-_{\rightarrow})^*(B^+_{\leftarrow} + B^-_{\leftarrow})}{-ik^-_{2y}}(e^{-2ik^-_{2y}d_{\mathrm{SO}}} - 1)\right). \end{aligned} \tag{A4}$$

This equation is valid when both $k^+_{2y}$ and $k^-_{2y}$ are real. In the case when one of them is imaginary ($k^+_{1y}$ in the expression below) one has

$$\begin{aligned} N_2 &= d_{\mathrm{SO}}(|B^+_{\rightarrow} + B^-_{\rightarrow}|^2 + |B^+_{\leftarrow} + B^-_{\leftarrow}|^2) \\ &+|B^+_{\rightarrow} - B^-_{\rightarrow}|^2\left(\frac{1}{-2\kappa^+_{2y}}(e^{-2\kappa^+_{2y}d_{\mathrm{SO}}} - 1)\right) \\ &+|B^+_{\leftarrow} - B^-_{\leftarrow}|^2\left(\frac{1}{2\kappa^+_{2y}}(e^{2\kappa^+_{2y}d_{\mathrm{SO}}} - 1)\right) \\ &+2d_{\mathrm{SO}}\mathrm{Re}[(B^-_{\rightarrow} - B^-_{\rightarrow})^*(B^-_{\leftarrow} - B^-_{\leftarrow})] \\ &+\mathrm{Re}\left(\frac{(B^+_{\rightarrow} + B^-_{\rightarrow})^*(B^+_{\leftarrow} + B^-_{\leftarrow})}{-ik^-_{2y}}(e^{-2ik^-_{2y}d_{\mathrm{SO}}} - 1)\right). \end{aligned} \tag{A5}$$

Here $\kappa^+_{2y} = |k^+_{2y}|$. Changing + and − we obtain the expression for $N_2$ when $k^+_{2y}$ is real and $k^-_{2y}$ is imaginary.

When both $k^+_{2y}$ and $k^-_{2y}$ are imaginary we find

$$\begin{aligned} N_2 &= |B^+_{\rightarrow} - B^-_{\rightarrow}|^2\left(\frac{1}{-2\kappa^+_{2y}}(e^{-2\kappa^+_{2y}d_{\mathrm{SO}}} - 1)\right) \\ &+|B^+_{\rightarrow} + B^-_{\rightarrow}|^2\left(\frac{1}{-2\kappa^-_{2y}}(e^{-2\kappa^-_{2y}d_{\mathrm{SO}}} - 1)\right) \\ &+|B^+_{\leftarrow} - B^-_{\leftarrow}|^2\left(\frac{1}{2\kappa^+_{2y}}(e^{2\kappa^+_{2y}d_{\mathrm{SO}}} - 1)\right) \\ &+|B^+_{\leftarrow} + B^-_{\leftarrow}|^2\left(\frac{1}{2\kappa^-_{2y}}(e^{2\kappa^-_{2y}d_{\mathrm{SO}}} - 1)\right) \\ &+2d_{\mathrm{SO}}\mathrm{Re}[(B^-_{\rightarrow} - B^-_{\rightarrow})^*(B^-_{\leftarrow} - B^-_{\leftarrow})] \\ &+2d_{\mathrm{SO}}\mathrm{Re}[(B^-_{\rightarrow} + B^-_{\rightarrow})^*(B^-_{\leftarrow} + B^-_{\leftarrow})]. \end{aligned} \tag{A6}$$

## APPENDIX B: MATRIX ELEMENT OF SOI FOR THE WAVE FUNCTION OF THIN FILM SYSTEM

When $k^+_{2y}$ is imaginary ($\kappa^+_{2y} = |k^+_{2y}|$) and $k^-_{2y}$ is real we have

$$\begin{aligned} W^{(i)}_{\mathrm{SO}} &= I\Big(-\kappa^+_{2y}\left(k_x + \frac{q}{2}\right)|B^+_{\rightarrow} - B^-_{\rightarrow}|^2 e^{-2\kappa^+_{2y}y_i} + \kappa^+_{2y} \\ &\times \left(k_x - \frac{q}{2}\right)|B^+_{\leftarrow} - B^-_{\leftarrow}|^2 e^{2\kappa^+_{2y}y_i} + 2\mathrm{Re}(ik^-_{2y}(k_x + q/2) \\ &\times (B^+_{\rightarrow} + B^-_{\rightarrow})^*(B^+_{\leftarrow} + B^-_{\leftarrow})e^{-2ik^-_{2y}y_i})\Big). \end{aligned} \tag{B1}$$

In the opposite case

$$\begin{aligned} W^{(i)}_{\mathrm{SO}} &= I\Big(\kappa^-_{2y}\left(k_x + \frac{q}{2}\right)|B^+_{\rightarrow} + B^-_{\rightarrow}|^2 e^{-2\kappa^-_{2y}y_i} \\ &- \kappa^-_{2y}\left(k_x + \frac{q}{2}\right)|B^+_{\leftarrow} + B^-_{\leftarrow}|^2 e^{2\kappa^-_{2y}y_i} \\ &- 2\mathrm{Re}(ik^+_{2y}(k_x - q/2)(B^+_{\rightarrow} - B^-_{\rightarrow})^* \\ &\times (B^+_{\leftarrow} - B^-_{\leftarrow})e^{-2ik^+_{2y}y_i})\Big). \end{aligned} \tag{B2}$$

When both quasimomentums are imaginary one has

$$\begin{aligned} W^{(i)}_{\mathrm{SO}} &= I\Big(\kappa^-_{2y}\left(k_x + \frac{q}{2}\right)|B^+_{\rightarrow} + B^-_{\rightarrow}|^2 e^{-2\kappa^-_{2y}y_i} \\ &- \kappa^-_{2y}\left(k_x + \frac{q}{2}\right)|B^+_{\leftarrow} + B^-_{\leftarrow}|^2 e^{2\kappa^-_{2y}y_i} \\ &-, \kappa^+_{2y}\left(k_x - \frac{q}{2}\right)|B^+_{\rightarrow} - B^-_{\rightarrow}|^2 e^{-2\kappa^+_{2y}y_i} \\ &+ \kappa^+_{2y}\left(k_x - \frac{q}{2}\right)|B^+_{\leftarrow} - B^-_{\leftarrow}|^2 e^{2\kappa^+_{2y}y_i}\Big). \end{aligned} \tag{B3}$$


[1] C. Moreau-Luchaire, C. Moutafis, N. Reyren, J. Sampaio, C. A. F. Vaz, N. V. Horne, K. Bouzehouane, K. Garcia, C. Deranlot, P. Warnicke, P. Wohlhüter, J.-M. George, M. Weigand, J. Raabe, V. Cros, and A. Fert, Nat. Nanotechnol. **11**, 444 (2016).

[2] X. Ma, G. Yu, X. Li, T. Wang, D. Wu, K. S. Olsson, Z. Chu, K. An, J. Q. Xiao, K. L. Wang, and X. Li, Phys. Rev. B **94**, 180408(R) (2016).

[3] B. Dupé, G. Bihlmayer, M. Böttcher, S. Blügel, and S. Heinze, Nat. Commun. **7**, 11779 (2016).

[4] M. Belmeguenai, J.-P. Adam, Y. Roussigné, S. Eimer, T. Devolder, J.-V. Kim, S. M. Cherif, A. Stashkevich, and A. Thiaville, Phys. Rev. B **91**, 180405(R) (2015).
[5] A. Soumyanarayanan, M. Raju, A. L. G. Oyarce, A. K. C. Tan, M.-Y. Im, A. P. Petrović, P. Ho, K. H. Khoo, M. Tran, C. K. Gan, F. Ernult, and C. Panagopoulos, Nat. Mater. **16**, 898 (2017).
[6] K. Di, V. L. Zhang, H. S. Lim, S. C. Ng, M. H. Kuok, J. Yu, J. Yoon, X. Qiu, and H. Yang, Phys. Rev. Lett. **114**, 047201 (2015).
[7] A. L. Balk, K.-W. Kim, D. T. Pierce, M. D. Stiles, J. Unguris, and S. M. Stavis, Phys. Rev. Lett. **119**, 077205 (2017).
[8] A. W. J. Wells, P. M. Shepley, C. H. Marrows, and T. A. Moore, Phys. Rev. B **95**, 054428 (2017).
[9] R. Lavrijsen, D. M. F. Hartmann, A. van den Brink, Y. Yin, B. Barcones, R. A. Duine, M. A. Verheijen, H. J. M. Swagten, and B. Koopmans, Phys. Rev. B **91**, 104414 (2015).
[10] H. Jia, B. Zimmermann, and S. Blügel, Phys. Rev. B **98**, 144427 (2018).
[11] K. Everschor-Sitte, J. Masell, R. M. Reeve, and M. Kläui, J. Appl. Phys. **124**, 240901 (2018).
[12] W. Jiang, P. Upadhyaya, W. Zhang, G. Yu, M. B. Jungfleisch, F. Y. Fradin, J. E. Pearson, Y. Tserkovnyak, K. L. Wang, O. Heinonen, S. G. E. te Velthuis, and A. Hoffmann, Science **349**, 283 (2015).
[13] N. Romming, C. Hanneken, M. Menzel, J. E. Bickel, B. Wolter, K. von Bergmann, A. Kubetzka, and R. Wiesendanger, Science **341**, 636 (2013).
[14] G. Yu, P. Upadhyaya, Q. Shao, H. Wu, G. Yin, X. Li, C. He, W. Jiang, X. Han, P. K. Amiri, and K. L. Wang, Nano Lett. **17**, 261 (2017).
[15] J. Ding, X. Yang, and T. Zhu, J. Phys. D **48**, 115004 (2015).
[16] G. Finocchio, F. Buttner, R. Tomasello, M. Carpentieri, and M. Klaui, J. Phys. D **49**, 423001 (2016).
[17] P.-J. Hsu, A. Kubetzka, A. Finco, N. Romming, K. von Bergmann, and R. Wiesendanger, Nat. Nanotechnol. **12**, 123 (2017).
[18] Y. Liu, N. Lei, C. Wang, X. Zhang, W. Kang, D. Zhu, Y. Zhou, X. Liu, Y. Zhang, and W. Zhao, Phys. Rev. Appl. **11**, 014004 (2019).
[19] K. Nawaoka, S. Miwa, Y. Shiota, N. Mizuochi, and Y. Suzuki, Appl. Phys. Express **8**, 063004 (2015).
[20] W. Zhang, H. Zhong, R. Zang, Y. Zhang, S. Yu, G. Han, G. L. Liu, S. S. Yan, S. Kang, and L. M. Mei, Appl. Phys. Lett. **113**, 122406 (2018).
[21] T. Srivastava, M. Schott, R. Juge, V. Křižáková, M. Belmeguenai, Y. Roussigné, A. Bernand-Mantel, L. Ranno, S. Pizzini, S.-M. Chérif, A. Stashkevich, S. Auffret, O. Boulle, G. Gaudin, M. Chshiev, C. Baraduc, and H. Béa, Nano Lett. **18**, 4871 (2018).
[22] N. S. Gusev, A. V. Sadovnikov, S. A. Nikitov, M. V. Sapozhnikov, and O. G. Udalov, Phys. Rev. Lett. **124**, 157202 (2020).
[23] A. Fert and P. M. Levy, Phys. Rev. Lett. **44**, 1538 (1980).
[24] H. Jia, B. Zimmermann, G. Michalicek, G. Bihlmayer, and S. Blügel, Phys. Rev. Mater. **4**, 024405 (2020).
[25] K.-W. Kim, H.-W. Lee, K.-J. Lee, and M. D. Stiles, Phys. Rev. Lett. **111**, 216601 (2013).
[26] H. Imamura, P. Bruno, and Y. Utsumi, Phys. Rev. B **69**, 121303(R) (2004).
[27] A. Kundu and S. Zhang, Phys. Rev. B **92**, 094434 (2015).
[28] S. Tacchi, R. E. Troncoso, M. Ahlberg, G. Gubbiotti, M. Madami, J. Åkerman, and P. Landeros, Phys. Rev. Lett. **118**, 147201 (2017).
[29] A. Crepieux and C. Lacroix, J. Magn. Magn. Mater. **182**, 341 (1998).
[30] S. V. Vonsovskii, *Magnetism* (Wiley, New York, 1974).
[31] C. M. Singal and T. P. Das, Phys. Rev. B **16**, 5068 (1977).
[32] F. J. Himpsel and D. E. Eastman, Phys. Rev. B **21**, 3207 (1980).
[33] S. Wakoh and J. Yamashita, J. Phys. Soc. Jpn. **28**, 1151 (1970).
[34] H. Yang, A. Thiaville, S. Rohart, A. Fert, and M. Chshiev, Phys. Rev. Lett. **115**, 267210 (2015).
[35] W. Köster and H. Franz, Metall. Rev. **6**, 1 (1961).